Desorption-induced first-order phase transition in a cyano-bridged compound

Y. Moritomo,[1,a)] F. Nakada,[1] H. Kamioka,[1] J. E. Kim,[2] and M. Takata[3]
[1]*Department of Physics, University of Tsukuba, Tsukuba 305-8571, Japan*
[2]*JASRI/SPring-8, 1-1-1 Kouto, Sayo-cho, Sayo-gun, Hyogo 679-5198, Japan*
[3]*RIKEN/SPring-8, 1-1-1 Kouto, Sayo-cho, Sayo-gun, Hyogo 679-5148, Japan*

(Received 20 February 2008; accepted 20 March 2008; published online 8 April 2008)

The *guest-host* interaction is one of the promising tools to control the material state. Here, we found that a cyano-bridged compound $Na_{0.50}Co[Fe(CN)_6]_{0.72}3.8H_2O$ shows a first-order structural phase transition below a critical pressure P_c (150 Pa) at 300 K. Judging from suppression of the OH stretching mode in the infrared spectra, we ascribed the phase transition to desorption of the ligand waters. The phase transition accompanies a significant change of the visible absorption spectra, reflecting the strong hybridization between the Co e_g state and the CNσ states. © *2008 American Institute of Physics*. [DOI: 10.1063/1.2908049]

Recently, nanoporous compounds are attracting the interest of materials scientists because the nanospaces of the host compound can be utilized as storage of the guest molecules, such as O_2, H_2O, NO, and so on.[1] In an extreme case, the low-dimensional alignment of the nanospaces induces an interesting physical property of the guest molecules. For example, one-dimensional arrangement of O_2 within the framework of a copper coordination polymer, $[Cu_2(pzdc)_2(pyz)]_n$, causes a spin gap behavior.[2] Another significant feature of the nanoporous material is the *guest-host* interaction, which may change the lattice structure[3] as well as the electronic and magnetic properties of the host system. In this letter, we report the desorption-induced first-order phase transition of the host framework in a cyano-bridged transition metal compound.

The cyano-bridged compound, $Na_xCo[Fe(CN)_6]_yzH_2O$, is a nanoporous material. The compound consists of a three-dimensional host framework,–NC–Fe–CN–Co–NC–, and the guest species, that is, alkaline metals and waters. A part of the waters locates at the $[Fe(CN)_6]$ vacancies and coordinates the Co ion (ligand water). The residual waters (zeolite water) and the alkaline metals locate in the nanospaces of the host framework. A significant feature of the cyano-bridged compound is the controllability of the guest concentration by electrochemical process,[4] humidity[5] and so on. Especially, the valence state of the transition metal can be tuned by the Na concentration (x), analogous to the case of the chemical hole doping in the transition metal oxides. The Co–Fe compound is attracting the interest of material scientists because it shows the photoinduced magnetization[6,7] and the photoinduced structural change.[8]

Films of the Co–Fe compound were electrochemically synthesized on indium tin oxide (ITO) transparent electrodes (sheet resistance was 100 Ω) under potentiostatic condition at −0.5 V versus a standard Ag/AgCl electrode in an aqueous solution containing 0.5 mmol/l $K_3[Fe^{II}(CN)_6]$, 1.25 mmol/l $Co^{II}(NO_3)_2$, and 1 mol/l $Na(NO_3)$. The elemental analysis by the inductively coupled plasma method and a CNH organic elementary analyzer (Perkin–Elmer 2400 CHN Elemental Analyzer) yields $Na_{0.88}Co[Fe(CN)_6]_{0.70}3.8H_2O$ (x=0.88). The film thickness was about 500 nm, which was determined by the cross-sectional scanning electron microscope image. We further control x by the oxidization process of the film at 0.5–0.7 V versus a standard Ag/AgCl electrode in 1 mol $Na(NO_3)$ aqueous solution. Here, we found that x decreases in proportion to the total charge (electrons/Co site) flown in the oxidation process, while the $[Fe(CN)_6]$ concentration (y=0.69–0.72) and the water concentration (z=0.38) are nearly unchanged. The chemical composition of the films are $Na_{0.50}Co[Fe(CN)_6]_{0.72}3.8H_2O$ (x=0.50) and $Na_{0.30}Co[Fe(CN)_6]_{0.72}3.8H_2O$ (x=0.30). The x-ray powder diffraction patterns are consistent with the face-centered cubic, the lattice constant is 1.030 24(1) nm at x=0.88 and 1.027 69(1) nm at x=0.50. The film color changes from transparent green to red with the decrease of x.

Figures 1 show the absorption spectra of these films in (a) infrared and (b) visible region. In the as-grown film (x=0.88), an intense absorption band is observed at 2080 cm^{-1}, which is ascribed to the stretching vibration of the CN moiety sandwiched by the low-spin Fe^{II} and the high-spin Co^{II}.[9] In the fullyoxidized film (x=0.30), an absorption band is observed at 2120 cm^{-1}, which is due to the CN moiety sandwiched by the low-spin Fe^{II} and the low-spin Co^{III}.[10] In the intermediate film (x=0.50), the absorption consists of two bands [see the least square-fitted broken curve of Fig.

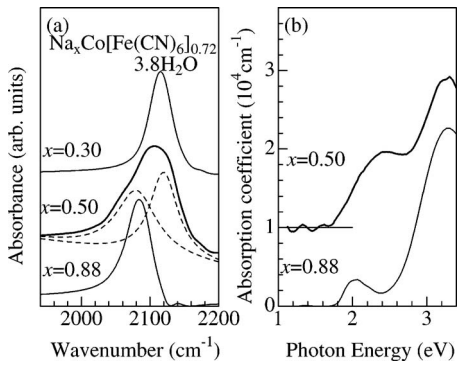

FIG. 1. (a) Infrared absorption spectra of $Na_xCo[Fe(CN)_6]_{0.72}3.8H_2O$. Broken curves are the result of the least-square-fitting with two Lorentz functions. (b) Visible absorption spectra of $Na_xCo[Fe(CN)_6]_{0.72}3.8H_2O$.

a)Electronic mail: moritomo@sakura.cc.tsukuba.ac.jp.

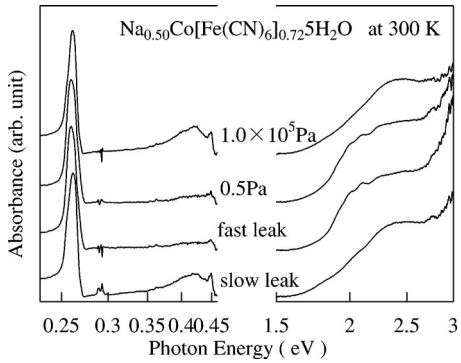

FIG. 2. Infrared and visible absorption spectra of $Na_{0.50}Co[Fe(CN)_6]_{0.72}3.8H_2O$ under various pressure conditions. A downward arrow indicates the OH stretching band. A broken curve in the left panel is the differential spectra between the ambient pressure spectrum and the vacuum spectrum.

1(a)], which indicates the coexistence of the low-spin Co^{III} and the high-spin Co^{II}. The valence modification also changes the visible absorption spectra. At $x=0.88$ [Fig. 1(b)], the spectra consists of the intense 3.2 eV band and the weak 2.0 eV band. At $x=0.50$, however, the 2.0 eV band disappears and a much stronger band appears at 2.4 eV. Ohkoshi *et al.*[5] reported a similar 2.0 eV band in $(Co^{II}_{0.41}Mn^{II}_{0.59})\times[Cr^{III}(CN)_6]_{2/3}4.2H_2O$ and ascribed it to the intra-atomic *d-d* transition of the four-coordinate tetrahedral Co^{II} site. On the other hand, the stronger 2.4 eV band at $x=0.50$ is ascribed to the charge-transfer excitation from the Fe^{II} site to the Co^{III} site. The 3.2 eV band is insensitive to x and is reasonably ascribed to the lignad-metal charge-transfer transition of $[Fe^{II}(CN)_6]$.

Figure 2 show the depressurization effect on the infrared and visible absorption spectra at $x=0.50$. The depressurization process significantly suppresses the OH stretching band at 0.43 eV (see the downward arrow in Fig. 2), indicating that waters are desorbed in vacuum.

The depressurization process further induces the 2 eV band, as seen in the differential spectrum (broken curve). These spectral changes are reversible in repeated pressure-cycles (see the bottom spectra of Fig. 2). The desorption process of the water molecules takes a few minutes, while the adsorption process takes a few hours. We investigated the depressurization effect on the electronic state of the Fe and Co ions by means of the x-ray absorption near edge structure (XANES) around the *K*-edge region at 300 K and found that only the Co spectrum shows a detectable change. Therefore, we ascribed the desorption-induced 2 eV band to the intra-atomic *d-d* transition of the Co^{II} site and call the band as "Co^{II} band."

To quantitatively investigate the depressurization effect on the spectral change, we measured the spectra at each pressure in the pressure-increasing run. The respective spectrum was measured after waiting for 5–10 min. We plotted in Fig. 3 the pressuredependence of the spectral weights for (a) the Co^{II} band (I_{Co}), (b) the OH stretching band (I_{OH}), and (c) the two CN stretching bands (I_{CN}). The magnitude of I_{Co} remains nearly constant ($\sim$0.75) below 10 Pa and then steeply decreases to $\sim$0.3. The reduction of I_{Co} is completed at a critical pressure P_c (150 Pa), showing a kink structure. Similar kink structures are observed in the P-I_{OH} curve [Fig. 3(b)] and the two P-I_{CN} curves [Fig. 3(c)] as indicated by the broken straight lines.

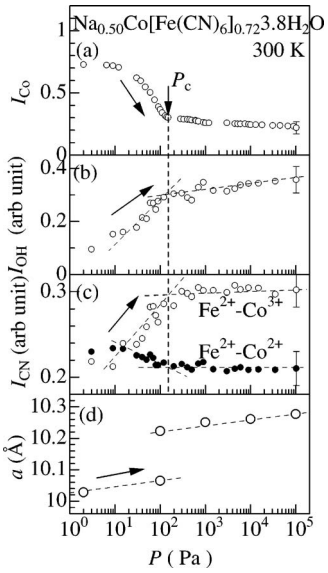

FIG. 3. Pressure dependence of the spectral weights for (a) the Co^{II} band (I_{Co}), (b) the OH stretching band (I_{OH}), and (c) the two CN stretching bands (I_{CN}) in $Na_{0.50}Co[Fe(CN)_6]_{0.72}3.8H_2O$ ($x=0.50$). (d) Pressure-dependence of the lattice constant *a*. The intensity of the Co^{II} band is normalized by that at $x=0.88$. Broken straight lines are merely the guide for the eyes.

We further investigated the depressurization effect on the structure. In this measurement, the film was carefully removed from the ITO glass with a microspatula and then the ground fine powders were filled into the 0.1 mmϕ glass capillary. The capillary was depressurized at 2 Pa for 30 min and then kept at the respective pressure for 30–60 min to reach an equilibrium state. Then, the capillary was sealed up and was put on a Debye–Scherrer camera at the BL02B2 beamline[11] of SPring-8. The lattice constant *a* was refined by the Rietveld method, and was plotted in Fig. 3(d). With increase of pressure beyond 100 Pa, *a* discontinuously increases from 1.006 nm to 1.022 nm. We emphasize that the small-*a* phase (volume fraction is 0.37) and the large-*a* phase (0.63) coexists at 100 Pa. Thus, the desorption-induced phase transition is of the first-order, accompanying a significant structural change.

We think that the ligand waters play an essential role on the phase transition and the spectral change. First of all, appearance of the Co^{II} band can be ascribed to the asymmetric ligand field around the Co^{II} site. In the Fe–Co cyanide, the e_g orbital strongly hybridized with the σ state of the ligands, that is, CN and H_2O.[12] Then, if the ligand waters are removed, the *d-d* transition of Co^{II} becomes dipole-allowed via the strong *d*-σ hybridization. Secondly, the ligand waters bear a part of the host framework. Then, desorption of the ligand waters causes reduction of the cell parameter. We, however, need a cooperative mechanism to explain the first-order nature of the phase transition. A most plausible mechanism may be the spin state transition of the Co^{II} site from the high-spin state ($S=3/2$) to the low-spin state ($S=1/2$). We measured the temperature dependence of the magnetic susceptibility of the sample sealed in the glass capillary and estimated the effective moment μ_{eff}. The magnitude of μ_{eff} decreases from 3.67 μ_B/Co at ambient pressure to 2.93 μ_B/Co at 3 Pa. This observation supports the idea of the spin state transition.

In conclusion, we observed vacuum-induced phase

transition (P_c=150 Pa) at 300 K in $Na_{0.50}Co[Fe(CN)_6]_{0.72}$ $3.8H_2O$. The phase transition is of the first-order and accompanies a significant spectral change in the visible region. Such a property can be utilized as the simple pressure marker. A systematic investigation with changing Na concentration (x), which is in progress, is significant to finely control the critical pressures.

This work was supported by a Grant-In-Aid for Scientific Research from the Ministry of Education, Culture, Sports, Science and Technology of Japan and the Japan Science and Technology Agency (CREST "X-ray Pinpoint Structural Measurement-Development of the Spatial- and Time-resolved Structural Study Technique for Nanomaterials and Devices"). We are grateful to Dr. Ohsawa for his help in the XANES spectroscopy. The synchrotron-radiation x-ray powder diffraction experiments were performed at the SPring-8 BL02B2 beamline with approval of the Japan Synchrotron Radiation Research Institute (JASRI).

[1] S. Kitagawa, R. Kitaura, and S. Noro, Angew. Chem., Int. Ed. **43**, 2334 (2004).
[2] R. Kitaura, S. Kitagawa, Y. Kubota, T. C. Kobayashi, K. Kindo, Y. Mita, A. Matsuo, M. Kobayashi, H.-C. Chang, T. C. Ozawa, M. Suzuki, M. Sakata, and M. Takata, Science **298**, 2358 (2002).
[3] O. M. Yaghi and H. Li, J. Am. Chem. Soc. **118**, 295 (1996).
[4] O. Sato, Y. Einaga, T. Iyoda, A. Fujishima, and K. Hashimoto, J. Phys. Chem. B **101**, 3903 (1997).
[5] S. Ohkoshi, K. Arai, Y. Sato, and K. Hashimoto, Nat. Mater. **3**, 857 (2004).
[6] O. Sato, T. Iyoda, A. Fujishima, and K. Hashimoto, Science **272**, 704 (1996).
[7] O. Sato, Y. Einaga, T. Iyoda, A. Fujishima, and K. Hashimoto, J. Electrochem. Soc. **144**, L11 (1997).
[8] M. Hanawa, Y. Moritomo, A. Kuriki, J. Tateishi, K. Kato, M. Takata, and M. Sakata, J. Phys. Soc. Jpn. **72**, 987 (2003).
[9] E. Reguera, J. F. Bertran, C. Diaz, and J. Blanco, Hyperfine Interact. **53**, 391 (1990).
[10] O. Sato, Y. Einaga, A. Fujishima, and K. Hashimoto, Inorg. Chem. **38**, 4405 (1999).
[11] E. Nishibori, M. Takata, K. Kato, M. Sakata, Y. Kubota, S. Aoyagi, Y. Kuroiwa, and M. Yamakawa, Nucl. Instrum. Methods Phys. Res. A **467-468**, 1045 (2001).
[12] T. Kawamoto, Y. Asai, and S. Abe, Phys. Rev. B **60**, 12990 (1999).